

Copyright WILEY-VCH Verlag GmbH & Co. KGaA, 69469 Weinheim, Germany, 2016.

Supporting Information

A Synergistic Na-Mn-O Composite Cathodes for High-Capacity Na-Ion Storage

Xuanpeng Wang,[†] Chenyang Wang,[†] Kang Han,[†] Chaojiang Niu, Jiashen Meng, Ping Hu, Xiaoming Xu, Zhaoyang Wang, Qi Li, Chunhua Han, ^{*} Yunhui Huang, Liqiang Mai^{*}

[†] These authors contributed equally to this work.

X. P. Wang, C. Y. Wang, K. Han, Dr. C. J. Niu, J. S. Meng, P. Hu, X. M. Xu, Z. Y. Wang, Dr. Q. Li, Dr. C. H. Han and Prof. L. Q. Mai

State Key Laboratory of Advanced Technology for Materials Synthesis and Processing,
Wuhan University of Technology, Wuhan 430070, China

Prof. Y. H. Huang

State Key Laboratory of Materials Processing and Die and Mould Technology, School of
Materials Science and Engineering , Huazhong University of Science and Technology ,
Wuhan 430074 , P. R. China.

Dong Guan McNair New Power Co., Ltd , Dong Guan 523000 , Guangdong , P. R. China.

E-mail: hch5927@whut.edu.cn, mlq518@whut.edu.cn

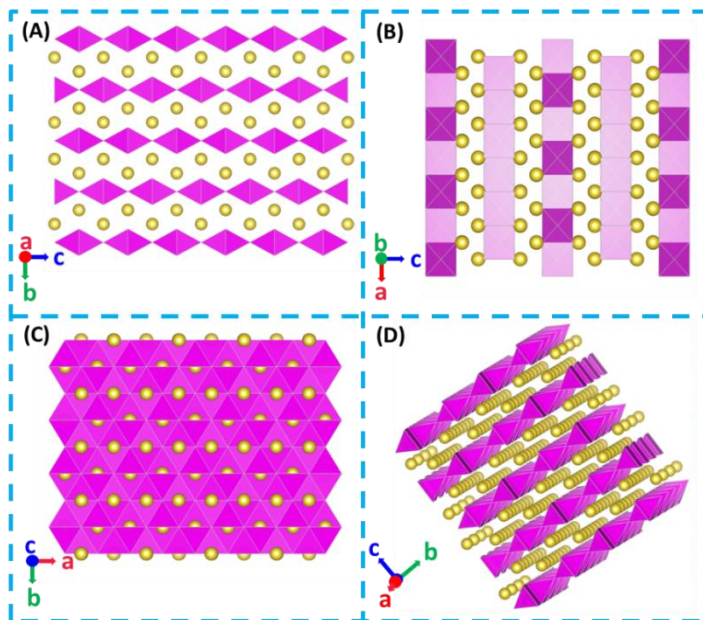


Figure S1. The crystal structure of orthorhombic $\text{Na}_4\text{Mn}_2\text{O}_5$.

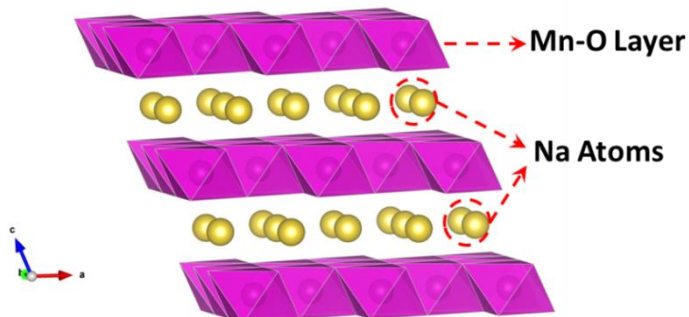


Figure S2. The crystal structure of layered $\text{Na}_{0.7}\text{MnO}_2$.

Table S1. The relation table of the Na:Mn ratio in initial state and final product.

Ratio of precursor	Na:Mn in precursor	Ratio of Na:Mn in final products	Ratio of $\text{Na}_4\text{Mn}_2\text{O}_5:\text{Na}_{0.7}\text{MnO}_2$
6:2		2.91:2.00	0.58:0.42
4:2		2.54:2.00	0.44:0.56
2:2		2.42:2.00	0.39:0.61

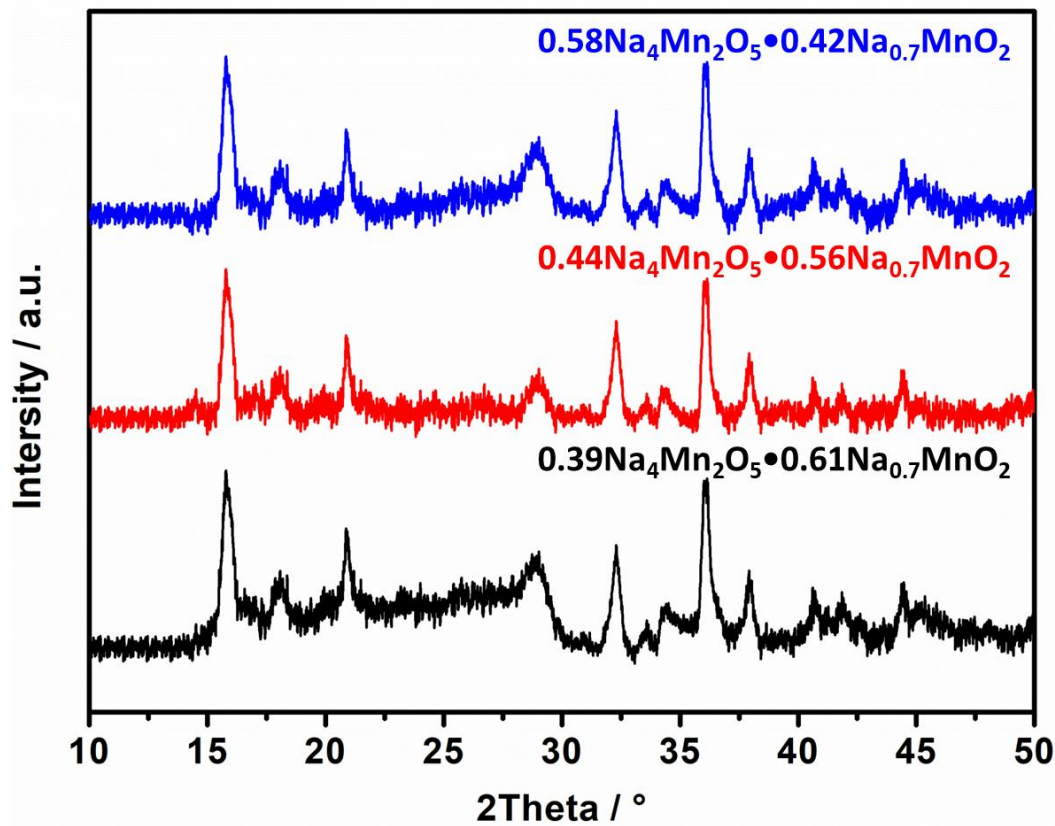


Figure S3. XRD patterns of the $0.58\text{Na}_4\text{Mn}_2\text{O}_5 \bullet 0.42\text{Na}_{0.7}\text{MnO}_2$, $0.44\text{Na}_4\text{Mn}_2\text{O}_5 \bullet 0.56\text{Na}_{0.7}\text{MnO}_2$ and $0.39\text{Na}_4\text{Mn}_2\text{O}_5 \bullet 0.61\text{Na}_{0.7}\text{MnO}_2$, respectively.

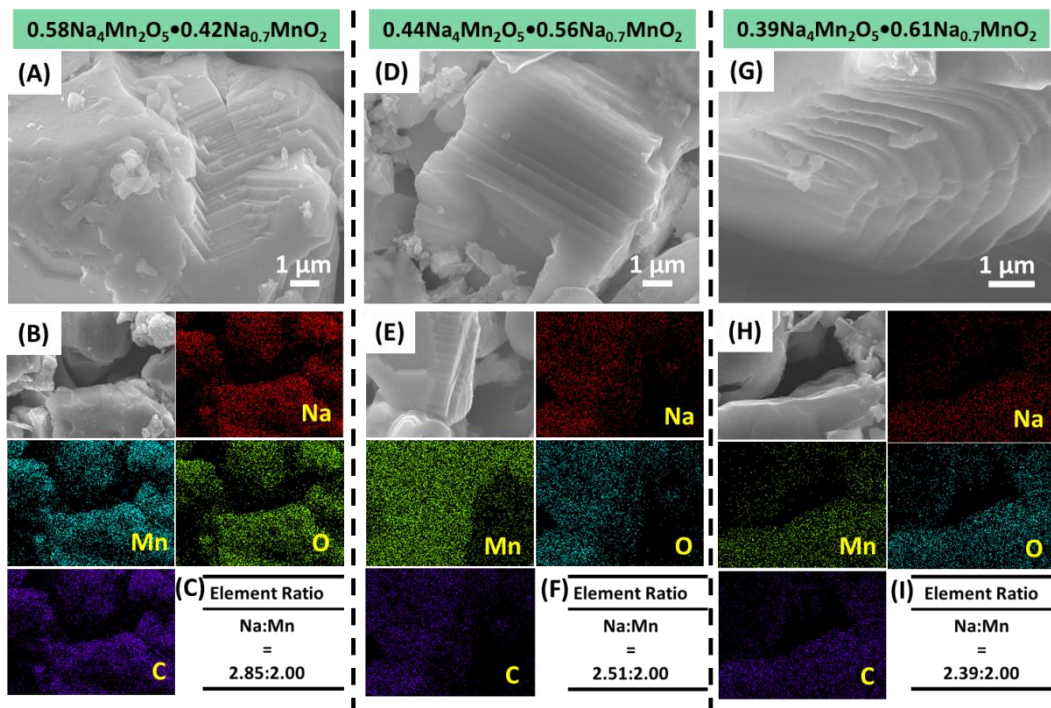


Figure S4. The SEM(A), EDS(B) and Na:Mn ratio (C) of $0.58\text{Na}_4\text{Mn}_2\text{O}_5 \bullet 0.42\text{Na}_{0.7}\text{MnO}_2$. The SEM(D), EDS(E) and Na:Mn ratio (F) of $0.44\text{Na}_4\text{Mn}_2\text{O}_5 \bullet 0.56\text{Na}_{0.7}\text{MnO}_2$. The SEM(G), EDS(H) and Na:Mn ratio (I) of $0.39\text{Na}_4\text{Mn}_2\text{O}_5 \bullet 0.61\text{Na}_{0.7}\text{MnO}_2$.

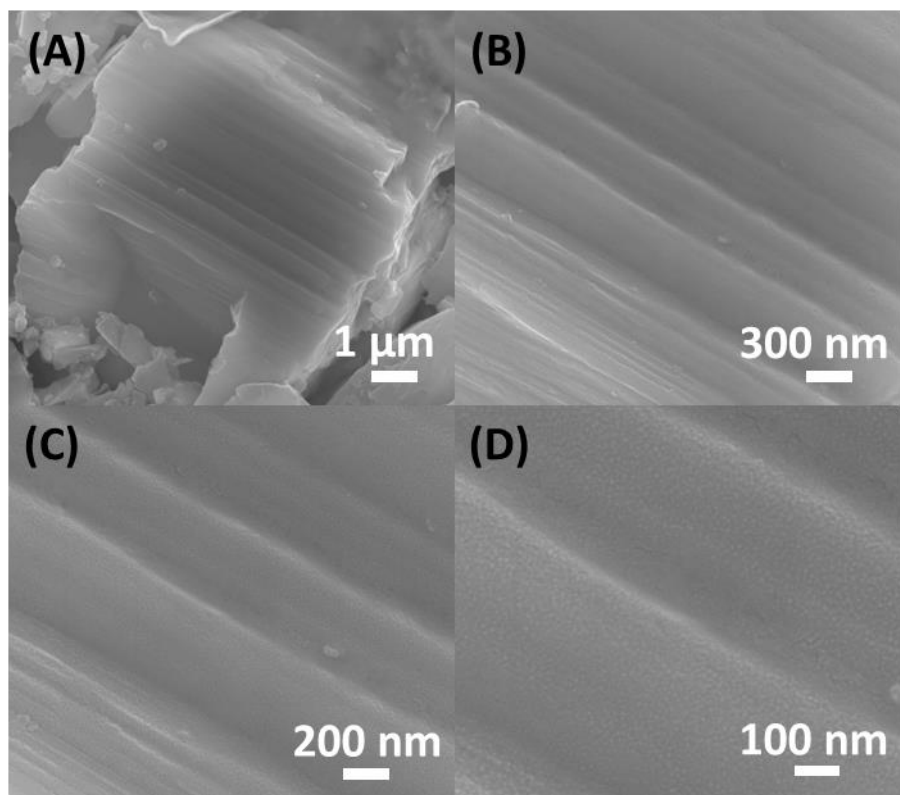


Figure S5. SEM images of the $0.44\text{Na}_4\text{Mn}_2\text{O}_5\bullet0.56\text{Na}_{0.7}\text{MnO}_2$.

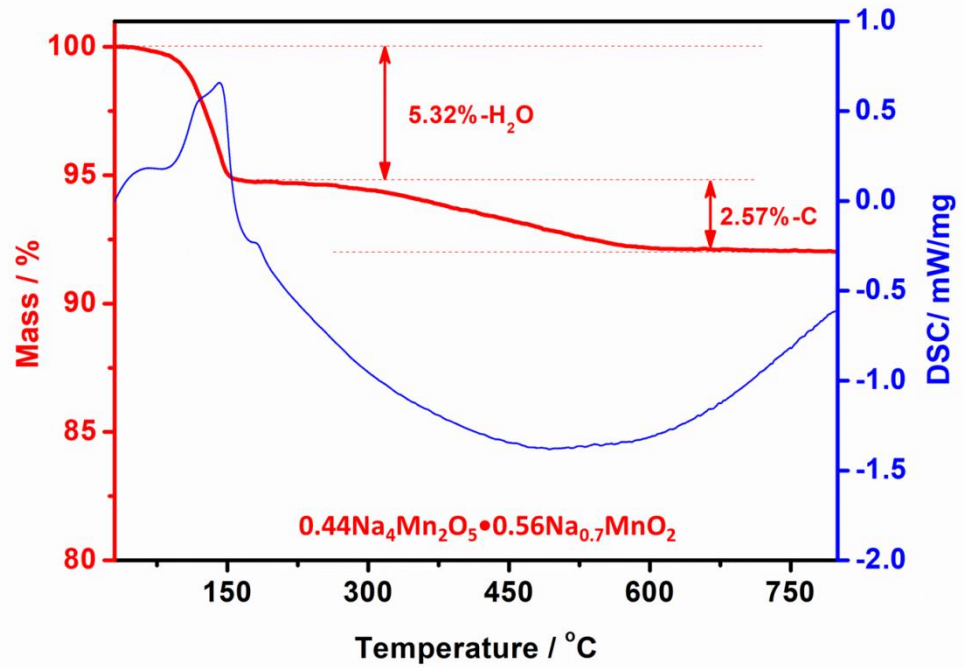


Figure S6. TG curves of the $0.44\text{Na}_4\text{Mn}_2\text{O}_5\bullet0.56\text{Na}_{0.7}\text{MnO}_2$.

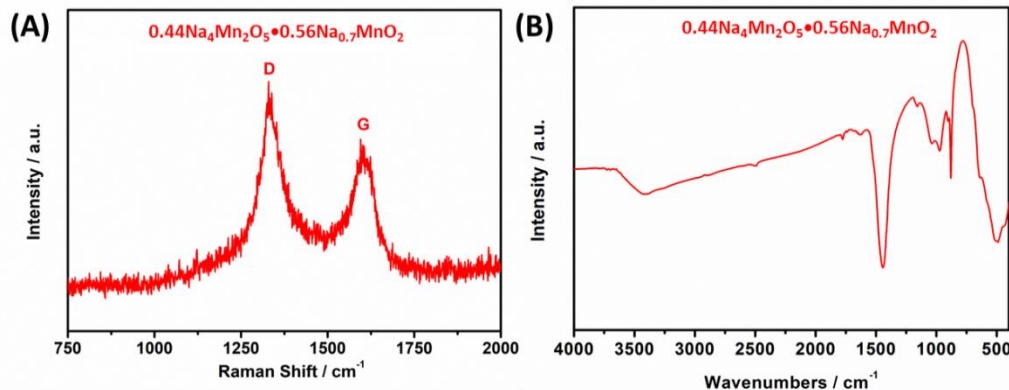


Figure S7. Raman spectra (A) and FT-IR (B) of the $0.44\text{Na}_4\text{Mn}_2\text{O}_5\bullet0.56\text{Na}_{0.7}\text{MnO}_2$.

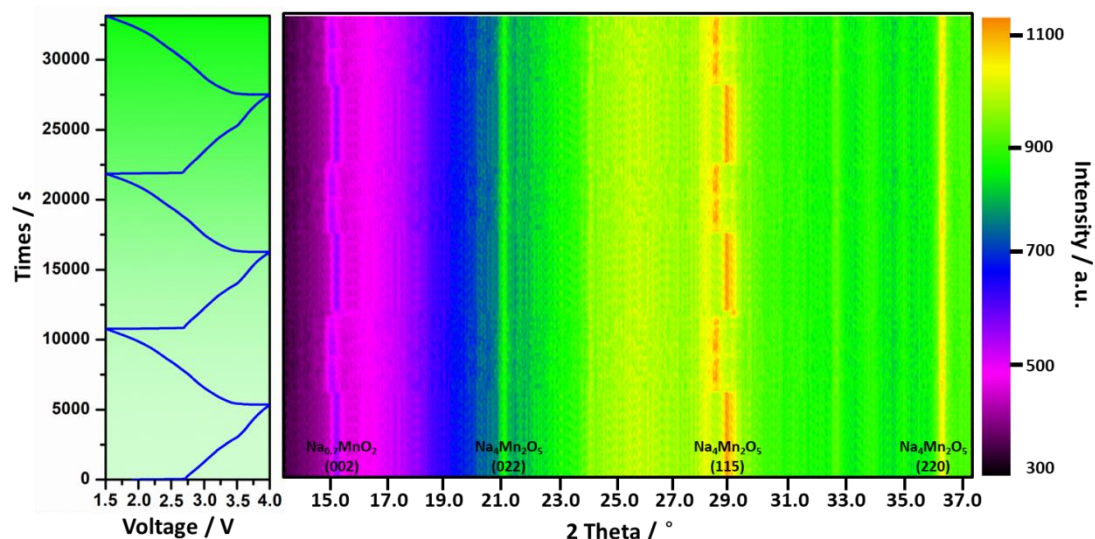


Figure S8. *In-situ* XRD patterns of $0.44\text{Na}_4\text{Mn}_2\text{O}_5\bullet0.56\text{Na}_{0.7}\text{MnO}_2$ during galvanostatic charge/discharge at 150 mA g^{-1} . The image plot of the XRD patterns at $13.5\text{--}37.2^\circ$ during the first three cycles.

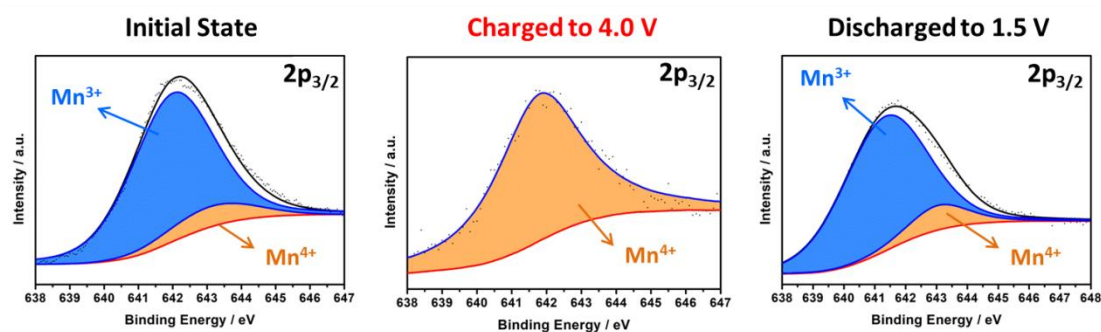


Figure S9. Charge/discharge curves of the $0.44\text{Na}_4\text{Mn}_2\text{O}_5\bullet0.56\text{Na}_{0.7}\text{MnO}_2$ at different current densities.

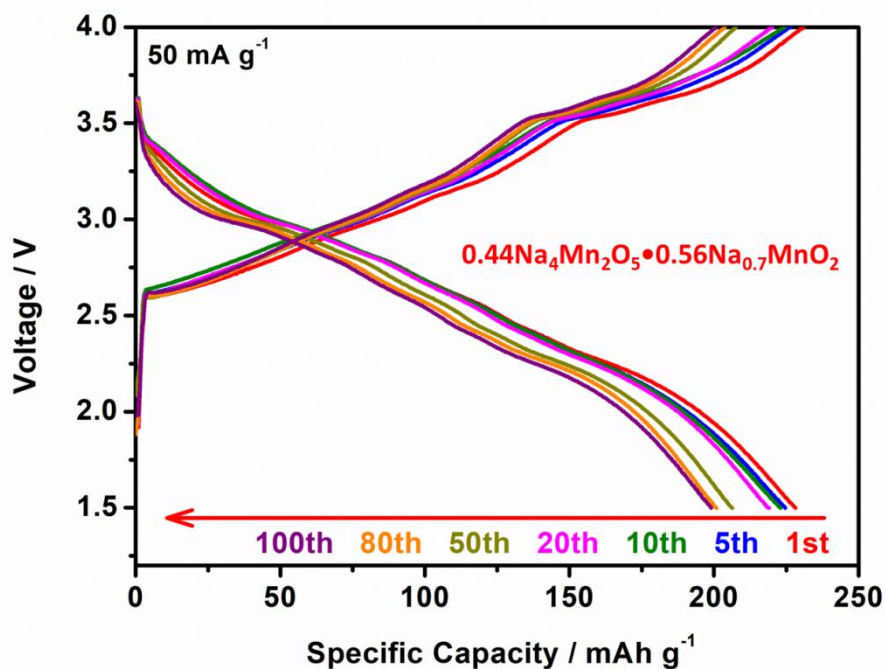


Figure S10. Charge/discharge curves of the $0.44\text{Na}_4\text{Mn}_2\text{O}_5 \bullet 0.56\text{Na}_{0.7}\text{MnO}_2$ at different cycles.

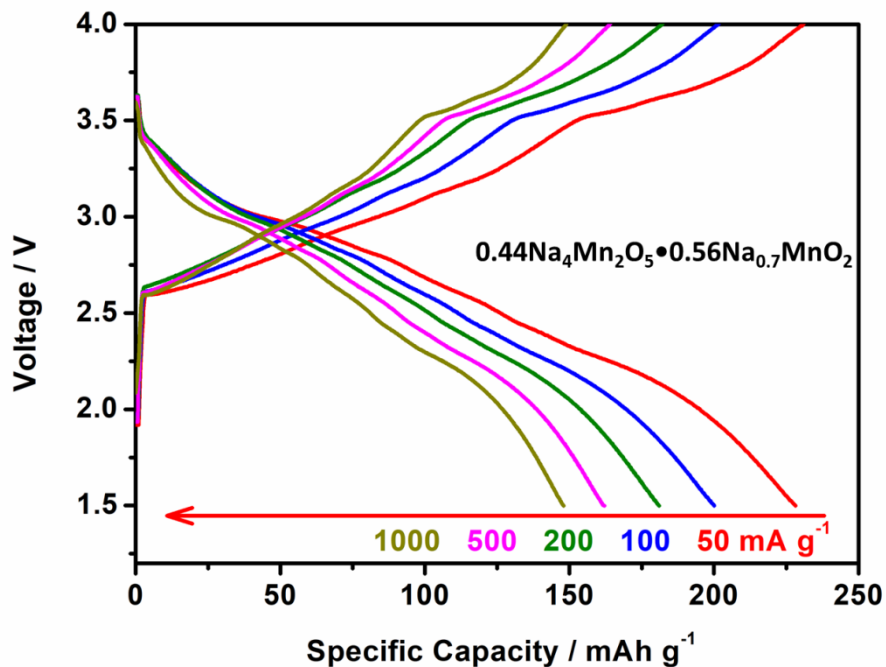


Figure S11. Charge/discharge curves of the $0.44\text{Na}_4\text{Mn}_2\text{O}_5 \bullet 0.56\text{Na}_{0.7}\text{MnO}_2$ at different current densities.

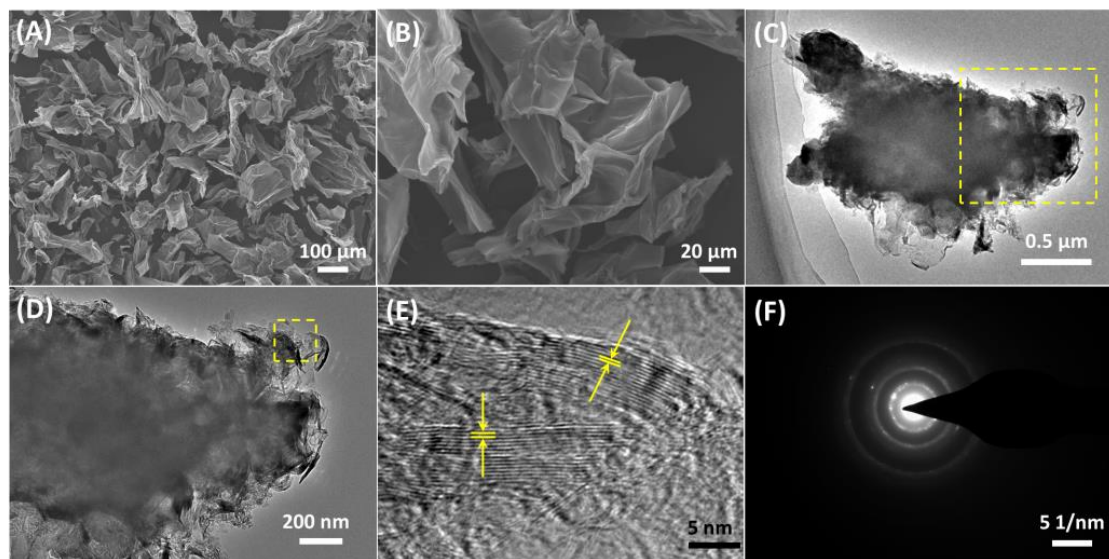


Figure S12. SEM images (A, B), TEM images (C, D), HR-TEM image (E) and SAED (F) of the hard carbon sintering at 1200 °C.

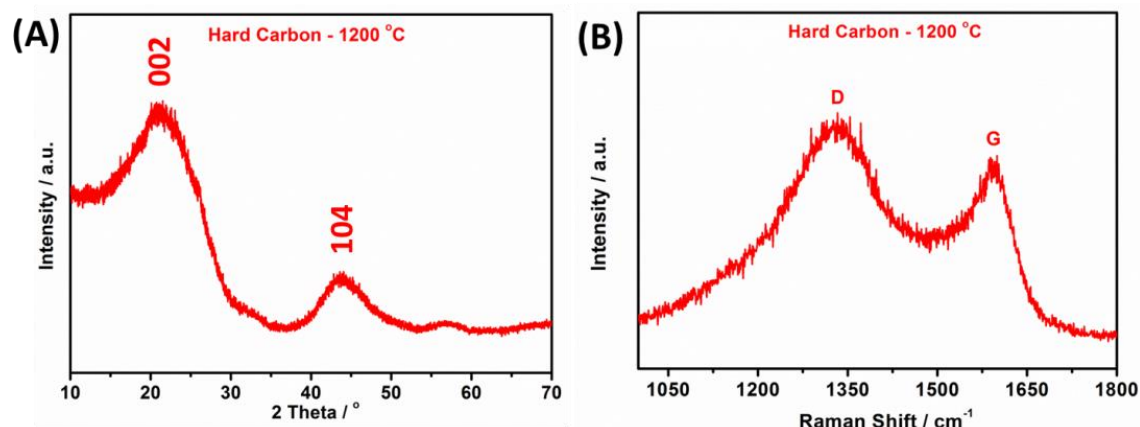


Figure S13. XRD spectrum (A) and Raman spectra (B) of the hard carbon sintering at 1200 °C.

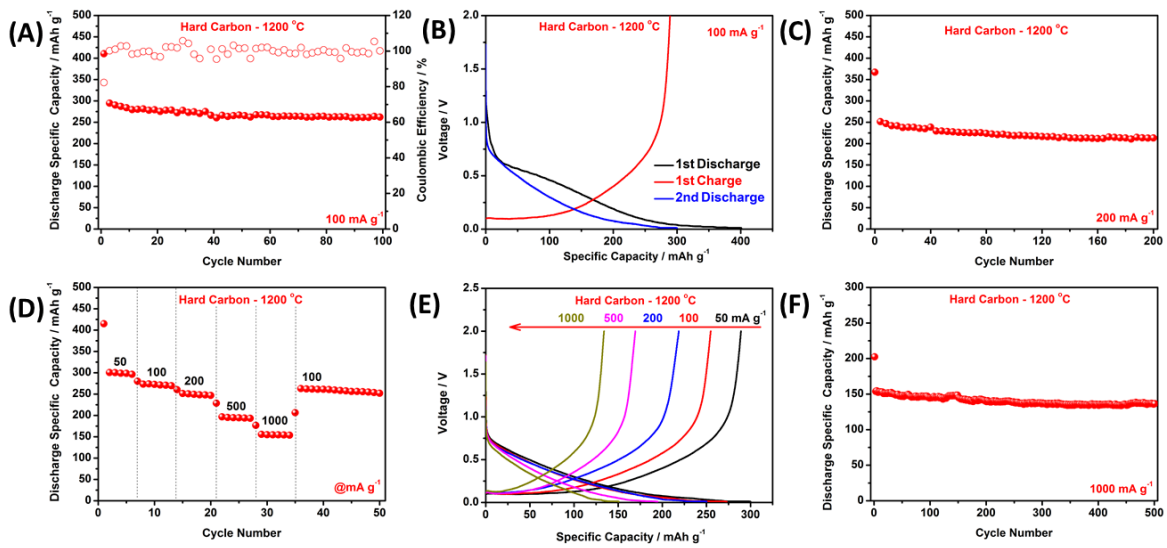


Figure S14. Characterization of electrochemical performance for hard carbon sintering at $1200 \text{ }^{\circ}\text{C}$ in NIBs. (A) Cyclic performance tested at 100 mA g^{-1} . (B) Charge/diacharge curves tested at 100 mA g^{-1} . (C) Cycling performance measured at 200 mA g^{-1} . (D) Rate performance. (E) Charge/diacharge curves tested different current densities. (F) Long-life cycling performance measured at 1000 mA g^{-1} .

Table S2. Comparison of the electrochemical performance of manganese-based cathode materials in LIBs and NIBs.

	Materials	Current Density (mA g ⁻¹)	Initial Capacity (mAh g ⁻¹)	Cycle Numbers	Capacity Retention	References
1	0.44Na₄Mn₂O₅•0.56Na_{0.7}MnO₂/Na Half Cells	50	228	100	87%	
		100	208	400	89%	
		1000	157	500	90%	Our work
2	0.44Na₄Mn₂O₅•0.56Na_{0.7}MnO₂/Hard Carbon Full Cells	50	151	100	86%	
		500	101	200	84%	
3	Li ₄ Mn ₂ O ₅ -LIBs	24.6	355	8	69%	[23]
4	Na _{0.6} (Li _{0.2} Mn _{0.8})O ₂ -NIBs	15	120	50	118%	[9]
5	Na _{0.66} Li _{0.18} Mn _{0.71} Ni _{0.21} Co _{0.08} O _{2+δ} -NIBs	50	150	150	75%	[24]
6	Na _{0.61} [Mn _{0.27} Fe _{0.34} Ti _{0.39}]O ₂ -NIBs	88	71	100	90%	[34]
7	β-NaMnO ₂ -NIBs	10	187	100	65%	[8]
8	Na _{0.7} Fe _{0.5} Mn _{0.5} O ₂ -NIBs	13	190	30	78%	[14]
9	K _{0.7} Fe _{0.5} Mn _{0.5} O ₂ -NIBs	100	181	100	93%	[19]
	Na[Ni _{0.58} Co _{0.06} Mn _{0.36}]O ₂ -NIBs	75	140.9	300	86%	[26]